

Simplicial minisuperspace. III. Integration contours in a five-simplex model

James B. Hartle

Department of Physics, University of California, Santa Barbara, California 93106

(Received 9 August 1988; accepted for publication 21 September 1988)

The no boundary proposal for the wave function of the universe is investigated in a minisuperspace model of pure gravity with cosmological constant. The model's four geometries consist of five four-simplices joined together to make the surface of a five-simplex from which one four-simplex face has been removed. The model is further simplified by symmetrically choosing all the interior edges of equal length and all the edges of the four-simplex boundary of equal length. The wave function is thus a function of a single boundary squared edge length and is specified by an integral over the single interior edge length. The analytic properties of the action in the space of complex edge lengths are exhibited, its classical extrema are calculated, and the possible contours of integration defining the wave function of the universe are discussed. A descending contour of constant imaginary action is proposed along which the integral defining the wave function is convergent and which predicts classical space-time in the late universe. This contour is the analog for the model of the conformally rotated contour appropriate to Euclidean sums over asymptotically flat space-times. The wave function is evaluated numerically for this contour both directly and by semiclassical methods.

I. INTRODUCTION

The "no boundary" proposal¹ for the initial conditions of our universe prescribes, among other amplitudes, the wave function of a closed universe on a connected spacelike surface as a Euclidean sum over histories of the form

$$\Psi_0(h, \phi, \partial M) = \sum_M \nu(M) \int_C \delta g \delta \Phi \exp(-I[g, \Phi, M]). \quad (1.1)$$

The arguments of the wave function, h and ϕ , denote the three metric and matter field configurations, respectively, on the three-manifold ∂M ; I is the Euclidean gravitational action for the metric g and matter field configurations Φ on a four-manifold M . The sum over manifolds is over a class of four-manifolds M that have a boundary ∂M and *no other boundary*. The functional integral is over the four-metrics g and matter field configurations Φ that induce h and ϕ , respectively, on the boundary ∂M . Other amplitudes are prescribed by this proposal. For example, there are the amplitudes associated with a surface that has disconnected parts,^{2,3} important for the value of the cosmological constant,⁴ or the "multisurface" amplitudes important for the recovery of a notion of time.⁵ These have an analogous construction to that of the wave function (1.1).

To make a construction such as (1.1) definite, the class of manifolds, the measure for the functional integrals, and the contour C over which these integrals are to be taken must all be specified. Various possibilities have been discussed for the class of manifolds^{2,6} and for the measure.⁷ In this paper we shall discuss some possibilities for the contour C in the context of a simplicial minisuperspace model.

For several reasons the contour of integration defining the wave function of the universe may be expected to run over complex metrics. First, were the action such as to make an integral over real metrics convergent, the wave function defined by (1.1) with a real contour of integration would contradict one of the immediate facts of our experience—the

classical space-time of the late universe. Classical space-time is a prediction of an oscillatory wave function in those regions of configuration space (the classically allowed regions) where it is well approximated semiclassically.^{2,8} The integral of $\exp(-I)$ over real Euclidean geometries can never oscillate. A complex contour is therefore necessary. Second, were the action such as to make an integral over real metrics convergent, it seems unlikely that (1.1) would yield a wave function satisfying the constraints required by diffeomorphism invariance and, in particular, the Wheeler-DeWitt equation.⁹ A complex contour of appropriate range could well give a construction by which the constraints are satisfied.

Fortunately, the Euclidean Einstein action—the low energy limit of any quantum theory of gravity—does not permit a real contour of integration with the unacceptable properties described above. It can assume arbitrarily negative values when evaluated on certain real metrics¹⁰ and (1.1) integrated over all real metrics would diverge. Merely from finiteness, one is naturally led to a complex contour.

In simple, familiar, flat space quantum field theories, there is no issue of the choice of contour for the Euclidean sum over histories defining the ground state. The sum is typically over real Euclidean field configurations with appropriate asymptotic behavior. Why then should the contour be an issue, or even a possibility for choice, for the sum over histories defining the analog of the ground state in the quantum mechanics of closed cosmologies? It is perhaps appropriate to briefly review the reasons.

Einstein gravity and gauge field theories are examples of theories that are most straightforwardly formulated in terms of redundant variables. Physical properties such as the positivity of the energy necessary for a stable ground state are features of the theory expressed in terms of these physical degrees of freedom. Sums over histories defining quantum amplitudes are sums over these physical degrees of freedom. Indeed, the machinery of gauge fixed functional integrals is a

formalism for carrying out just such sums without explicitly isolating the physical degrees of freedom. Redundant gauge degrees of freedom can be “fixed” in such constructions. However, if there are *gauge invariant* redundant degrees of freedom, there can be many contours of integration that correspond to summing the physical degrees of freedom over a real, physically appropriate range, but which differ in the contour assigned to the redundant variables. Such contours are physically equivalent when they give convergent results. It is the existence of gauge invariant redundant variables that makes the choice of contour an issue in (1.1).

Linearized general relativity is an example of a theory of this type for which the physical and redundant degrees can be explicitly identified. The action can be arbitrarily negative for some linearized metrics, but is positive when restricted to the physical degrees of freedom. The energy expressed in terms of the physical degrees of freedom is positive; therefore, there is a stable ground state. Indeed, it could not be otherwise since linearized gravity is just the theory of a free spin-2 field in flat space-time. The possible contours of integration for constructing the ground state wave function by the analog of (1.1) can be explicitly discussed.^{11,12} There is no real contour giving the ground state wave function since the resulting integral would be divergent. However, there are contours in which the redundant variables are integrated over complex values that correctly yield the ground state wave function of the Hamiltonian theory. Indeed, this can be demonstrated to all orders in perturbation theory.¹²

In the full theory of general relativity we have no explicit decomposition into physical and redundant variables. However, the positive energy theorem of classical general relativity¹³ suggests the existence of a stable ground state when the theory is restricted to asymptotically flat space-times. The work of Gibbons, Hawking, and Perry,¹⁰ coupled with the positive action theorem of Schoen and Yau¹⁴ has shown how sensible convergent results can be obtained for Euclidean sums over asymptotically flat space-times, with contours along which the conformal degree of freedom takes complex values. However, in the case of closed cosmologies we have, as yet, no explicit prescription for the complex contour that defines the “no boundary” wave functions. Here we have neither an explicit decomposition into physical and redundant variables nor a notion of total energy to guide us. Therefore, it seems appropriate to search *generally* for suitable contours. In particular, we can ask whether there are complex contours of integration that (i) are convergent, (ii) lead to a wave function that predicts classical space-time in the late ($t \gtrsim 10^{-43}$ sec) universe, and (iii) lead to a wave function that satisfies the constraints implementing diffeomorphism invariance. In this paper we discuss this question in the simplest simplicial minisuperspace model.

Minisuperspace models have a history of utility in the exploration of quantum gravity and quantum cosmology.^{15,16} In a minisuperspace model the parameters needed to describe a family of space-time histories is truncated to a manageable number leading to a tractable quantum mechanical model of general relativity. In some circumstances these models may give rise to approximations to quantities of physical interest.^{17,18} A useful class of systematically impro-

vable models can be obtained by using the methods of the Regge calculus,¹⁹ to restrict the geometries contributing to (1.1) to the possible simplicial geometries built on a fixed simplicial manifold. Such models were generally discussed in the first two papers of this series.^{18,20}

The question of the possible contours of integration obeying criteria (i)–(iii) can be usefully explored in minisuperspace models for which the possible contours can be explicitly displayed. Simplicial minisuperspace models are particularly useful in this way. The possible contours of integration are the contours in the space of complex squared edge lengths of the simplicial geometry. Since the Regge action is an *algebraic* function of the squared edge lengths, its analytic properties as a function of these many complex variables are straightforwardly displayed and the consequences of a particular choice of contour analyzed in an elementary way. In this paper we carry out such an analysis for the simplest minisuperspace model. The model is specified in Sec. II. In Sec. III the semiclassical approximation to the sum over geometries is discussed. In Sec. IV it is shown that the steepest descents contour through the extrema that give classical space-time in the late universe is a contour satisfying the applicable criteria above. Some brief conclusions are drawn in Sec. V.

II. THE MODEL

The surface of a tetrahedron (a three-simplex) consists of four triangles that together form a two-dimensional simplicial geometry without boundary. If one of these triangles is removed, the result is a two-dimensional simplicial geometry with a single one-dimensional boundary consisting of three edges (see Fig. 1). Two dimensions up, a similar procedure can be used to construct a four-dimensional simplicial geometry with a single S^3 boundary. A five-simplex consists of six points in five dimensions, with every pair defining an edge. The surface of a five-simplex consists of six four-simplices that together form a four-dimensional geometry without boundary. If one of these four-simplices is removed, the remaining five four-simplices form a simplicial four-geometry with a single three-sphere boundary. There are five vertices in the boundary and a single interior vertex. There are thus ten boundary edges and five interior ones that join the

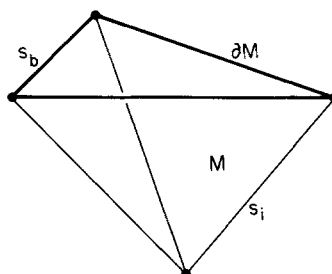


FIG. 1. A two-dimensional simplicial geometry. Remove one triangle from the surface of a tetrahedron and one obtains the two-dimensional simplicial geometry shown. The geometry consists of three triangles meeting in the single interior vertex. There is a single closed boundary consisting of the three edges (heavy lines) of the removed triangle. The simplicial geometry used in constructing the minisuperspace model of this paper is the four-dimensional analog of that pictured here.

interior vertex to each of the five boundary vertices (see Fig. 1). The simplicial manifold is clearly invariant under permutations of the five boundary vertices. If all boundary edges are chosen equal and all interior edges separately equal, one obtains a family of symmetric simplicial geometries. Each is characterized by just two numbers: the squared boundary edge length s_b , and the squared interior edge length s_i . This symmetric family of simplicial four-geometries defines our minisuperspace model. We include no other geometrical degrees of freedom, no other manifolds, and no matter degrees of freedom. The wave function is thus a function only of the boundary edge length s_b and given by the transcription of (1.1):

$$\Psi_0(s_b) = \int_C d\mu(s_i) \exp[-I(s_b, s_i)]. \quad (2.1)$$

The only integration is over the interior edge s_i over a contour C with a measure μ . To complete the model it remains to specify C , μ , and the action I .

For the action we take the Regge action for Euclidean Einstein gravity with cosmological constant, that is, we take the simplicial analog of

$$I^2 I = -2 \int_{\partial M} d^3x \sqrt{h} K - \int_M d^4x \sqrt{g} R + 2\Lambda \int_M d^4x \sqrt{g}. \quad (2.2)$$

Here, R is the scalar curvature, Λ is the cosmological constant, K is the extrinsic curvature scalar of the boundary, and $l = (16\pi G)^{1/2}$ is the Planck length in the units with $\hbar = c = 1$ used throughout. The first term is an integral over the boundary of the manifold and the second over its interior. The simplicial analog of (2.2) is^{19,21}

$$I^2 I = -2 \sum_{\sigma \in \partial M} A(\sigma) \psi(\sigma) - 2 \sum_{\sigma \in \text{int}(M)} A(\sigma) \theta(\sigma) + 2\Lambda \sum_{\tau \in \text{int}(M)} V_4(\tau). \quad (2.3)$$

The sums are, respectively, over triangles σ in the boundary ∂M , over triangles σ in the interior of M , and over interior four-simplices τ . Here, $\theta(\sigma)$ is the deficit angle of triangle σ and $\psi(\sigma)$ is the angle between the normals to the boundary tetrahedra meeting in triangle σ . The area of triangle σ is $A(\sigma)$ and $V_4(\tau)$ is the four-volume of the four-simplex τ . Further details of definition, as well as practical prescriptions for expressing these quantities in terms of squared edge lengths, are reviewed in Paper I.

The analytic properties of the action as a function of the complex squared edge lengths will be important for an analysis of possible complex contours of integration: Although they can be explicitly exhibited for the model, they are also generally read off easily from Eq. (2.3) and the relations (Paper I) defining volumes, areas, and angles in terms of squared edge lengths. In particular, let e_1, e_2, \dots, e_n be vectors lying along the edges of an n -simplex emanating from one chosen vertex 0. The volume n -form for the simplex is $\omega_n = e_1 \wedge \dots \wedge e_n$, and the squared volume is given in terms of it by [see Paper I, Eq. (3.6)]

$$V_n^2 = \omega_n \cdot \omega_n = [1/(n!)]^2 \det(e_\alpha \cdot e_\beta). \quad (2.4)$$

Since $e_\alpha \cdot e_\beta = (s_{0\alpha} + s_{0\beta} - s_{\alpha\beta})/2$, where $s_{\alpha\beta}$ is the squared

edge length between vertices α and β , we conclude that V_4^2 is a polynomial in the squared edge lengths. The deficit angle $\theta(\sigma)$ is 2π minus the sum of the "dihedral angles" between the three-simplices meeting at σ . Similarly, $\psi(\sigma)$ is π minus the sum of the dihedral angles between the interior three-simplices meeting at σ . The dihedral angle ϕ between two three-simplices with the volume forms ω_3 and ω'_3 is [see Paper I, Eq. (3.9)]

$$\phi = \cos^{-1}((\omega_3 \cdot \omega'_3)/V_3 V'_3) \quad (2.5)$$

and $\omega_3 \cdot \omega'_3 = (3!)^{-2} \det(e_\alpha \cdot e'_\beta)$. Using this formula, Eq. (2.4), the relation

$$\cos^{-1}(z) = -i \log(z + \sqrt{z^2 - 1}), \quad (2.6)$$

and the law of cosines to express the vector scalar products in terms of squared edge lengths, the analytic properties of the angles entering the action may be explicitly exhibited.

The analytic properties of the action in the complex squared edge lengths may be summarized as follows: There are logarithmic infinities on those surfaces that correspond to the vanishing of the polynomial which gives a three-simplex squared volume. The action is not single valued. Evidently, there are branch surfaces where the volume of a triangle, three-simplex, or four-simplex vanishes and, also, there are branch surfaces on which the squared cosine of any dihedral angle equals unity. However, a degenerate triangle or three-simplex implies the degeneracy of the four-simplex that contains it. Further, the identity [see Paper I, Eq. (3.12)]

$$\sin \phi = \frac{4}{3} A V_4 / V_3 V'_3 \quad (2.7)$$

gives a relation between the dihedral angle between two three-simplices meeting in a triangle, their volumes V_3 and V'_3 , the volume V_4 of the four-simplex they span, and the area A of the triangle in which they meet. This shows that $\cos \phi = \pm 1$ only when either A or V_4 vanishes. The branch surfaces of the action are therefore entirely contained in those surfaces on which the volume of some four-simplex vanishes. Except for these branch surfaces and logarithmic singularities the action is an analytic function of the squared edge lengths.

To carry out the integral (2.1) for the present model the action must be expressed in terms of the two edge lengths s_b and s_i . The quantities occurring in (2.3) are straightforwardly calculated by use of (2.4) and (2.5). The results are most conveniently expressed in terms of the dimensionless ratios

$$\xi = s_i/s_b, \quad S = H^2 s_b / l^2, \quad (2.8)$$

where $H^2 = l^2 \Lambda / 3$. The volume of each four-simplex is

$$V_4 = (1/(24\sqrt{2})) s_b^2 (\xi - \frac{1}{3})^{1/2}. \quad (2.9)$$

The area of each interior triangle is

$$A_i = \frac{1}{2} s_b (\xi - \frac{1}{4})^{1/2} \quad (2.10)$$

and the associated deficit angle is

$$\theta = 2\pi - 3 \cos^{-1} \{ \frac{1}{3} [(2\xi - 1)/(3\xi - 1)] \}. \quad (2.11)$$

The area of a boundary triangle is

$$A_b = (\sqrt{3}/4) s_b \quad (2.12)$$

and the angle ψ for each is

$$\psi = \pi - 2 \cos^{-1} \left\{ \frac{1}{(2\sqrt{2})} \left[\frac{1}{(3\xi - 1)^{1/2}} \right] \right\}. \quad (2.13)$$

The action (2.3) is then

$$I = [-S\mathcal{F}(\xi) + S^2\mathcal{G}(\xi)] / H^2 \equiv \mathcal{I}(S, \xi) / H^2, \quad (2.14)$$

where

$$\begin{aligned} \mathcal{F}(\xi) = & 5\{\sqrt{3} [\pi - 2 \cos^{-1}(z_1)] \\ & + (4\xi - 1)^{1/2} [2\pi - 3 \cos^{-1}(z_2)]\} \end{aligned} \quad (2.15)$$

and

$$\mathcal{G}(\xi) = (5\sqrt{2}/8)(\xi - \frac{3}{8})^{1/2}, \quad (2.16)$$

with

$$z_1 = \frac{1}{2\sqrt{2}} \frac{1}{(3\xi - 1)^{1/2}}, \quad z_2 = \frac{1}{2} \left(\frac{2\xi - 1}{3\xi - 1} \right). \quad (2.17)$$

In familiar quantum theories the choice of measure for a sum-over-histories formulation is dictated by requiring correspondence with the Hamiltonian version of the theory.⁶ However, there may be no natural Hamiltonian formulation of the quantum mechanics of closed cosmologies from which to draw this information.²² The corresponding constraints in the more general formulations of quantum mechanics have not yet been fully explored; they certainly have not been for the Regge calculus. Fortunately, the main results of this investigation for the contour C do not seem very sensitive to the choice of measure among those in a "reasonable" class, e.g., measures that are polynomials in the squared edge lengths. Several choices have been suggested as natural in one way or another. For illustrative purposes we shall choose the simplest possibility and write

$$d\mu(s_i) = ds_i / (2\pi i l^2). \quad (2.18)$$

The factor $2\pi i l^2$ is a convenient normalization. Thus we can write (2.1) as

$$\Psi_0(S) = \frac{S}{2\pi i H^2} \int_C d\xi \exp \left[- \frac{\mathcal{I}(S, \xi)}{H^2} \right]. \quad (2.19)$$

The analytic and asymptotic properties of the action $\mathcal{I}(S, \xi)$ as a function of the complex variable ξ are easily deduced from the general discussion of the analytic properties of the action or from the explicit expressions (2.9)–(2.13) and the definition of $\cos^{-1}(z)$. There is a square root branch point of $\mathcal{I}(S, \xi)$ at $\xi = \frac{3}{8}$ where the four-simplices become degenerate; there is another square root branch point at $\xi = \frac{1}{4}$ where the interior triangles become degenerate; and, finally, at $\xi = \frac{1}{3}$ there is a square root branch point and a logarithmic branch point near which $\mathcal{I}(S, \xi)$ behaves as

$$\mathcal{I}(S, \xi) \sim 10\sqrt{3} \log(3\xi - 1)S. \quad (2.20)$$

There is also a branch point of the logarithms at infinity.

Choosing phases so that $\cos^{-1}(z)$ is real for $-1 < z < 1$, real values of the squared edge length ξ correspond to real geometries with real metrics. Indeed, the metric inside each four-simplex is easily displayed in the basis whose defining basis vectors e_i lie along the edges from the single interior vertex 0 to the five vertices i of the boundary four-simplex; it is

$$g_{ij} = e_i \cdot e_j = \frac{1}{2}(s_{0i} + s_{0j} - s_{ij}), \quad (2.21)$$

where $s_{\alpha\beta}$ is the squared edge length joining vertices α and β . The metric is real for real values of $s_{\alpha\beta}$. For the symmetric choice of edges $s_{0i} = s_b \xi$ and $s_{ij} = s_b$, the eigenvalues of (2.21) are $\lambda = \frac{1}{2}$, $\lambda = \frac{1}{2}$, and the two values

$$\lambda = 1 + \frac{1}{2}\xi \pm \left[(1 + \frac{1}{2}\xi)^2 - 2(\xi - \frac{3}{8}) \right]^{1/2}. \quad (2.22)$$

Thus we have the signature $(+, +, +, +)$ for $\xi > \frac{3}{8}$ and $(-, +, +, +)$ for $\xi < \frac{3}{8}$. The real axis for $\xi > \frac{3}{8}$ is the regime of real Euclidean geometries; the regime for $\xi < \frac{3}{8}$ is the regime of real Lorentzian geometries.

The phases of the complex functions are chosen so that on the real axis for $\xi > \frac{3}{8}$ one has real volumes (2.9), real areas (2.10), real deficit angles (2.11), and real Euclidean action (2.14). It is thus convenient to define a first sheet for the action function cut from $\frac{3}{8}$ to $-\infty$. The reality of \mathcal{I} above $\xi = \frac{3}{8}$ establishes that the action is real analytic:

$$\overline{\mathcal{I}(S, \xi)} = \mathcal{I}(S, \xi). \quad (2.23)$$

The Euclidean action for the Lorentzian geometries in the range $\xi < \frac{1}{4}$ is pure imaginary, taking opposite signs above and below the cut. In this range, about the cut,

$$\begin{aligned} \mathcal{F}(\xi) = & i5 \left\{ -2\sqrt{3} \sinh^{-1} \left(\frac{1}{2\sqrt{2}(1-3\xi)^{1/2}} \right) \right. \\ & \left. + (1-4\xi)^{1/2} \right. \\ & \left. \times \left[2\pi - 3 \cos^{-1} \left(\frac{1}{2} \frac{2\xi-1}{3\xi-1} \right) \right] \right\}, \end{aligned} \quad (2.24a)$$

$$\mathcal{G}(\xi) = i(5\sqrt{2}/8) (\frac{3}{8} - \xi)^{1/2}. \quad (2.24b)$$

If the function $\mathcal{I}(S, \xi)$ is continued in ξ once around all the branch points at $\xi = \frac{1}{4}$, $\frac{1}{3}$, and $\frac{3}{8}$, that is, through the cut along $\xi < \frac{1}{4}$, we reach its second sheet. The value of $\mathcal{I}(S, \xi)$ on the second sheet is the negative of its value on the first sheet. This is easily seen as follows: The function $\cos^{-1}(z)$ defined by (2.6) has branch points at $z = -1$, $+1$, and ∞ and may be discussed in the plane cut from $-\infty$ to -1 and 1 to ∞ . The corresponding branch points of $\cos^{-1}(z_2)$ are at $\xi = \frac{3}{8}$, $\frac{1}{4}$, and $\frac{1}{3}$, respectively, so that the cuts defining its first sheet run from $\frac{1}{4}$ to $\frac{1}{3}$ and $\frac{1}{3}$ to $\frac{3}{8}$. Thus $\cos^{-1}(z_2)$ does not change when continued around $\xi = \frac{1}{4}$, $\frac{1}{3}$, and $\frac{3}{8}$. The branch points of $\cos^{-1}(z_1)$ corresponding to $z = -1$, 1 , and ∞ lie at $\xi = \frac{1}{4}$, $\frac{3}{8}$, and $\frac{1}{3}$, respectively, so again the cuts defining the first sheet lie between these points. Thus, from (2.17), when continued once around, $\cos^{-1}(z_1) \rightarrow \cos^{-1}(-z_1) = \pi - \cos^{-1}(z_1)$. These results, together with the changes in sign of the roots in (2.15) and (2.16), are sufficient to establish that $\mathcal{I}(S, \xi)$ on the second sheet is the negative of its value on the first sheet. In particular, if one continues twice around $\xi = \frac{1}{4}$, $\frac{1}{3}$, and $\frac{3}{8}$, the function $\mathcal{I}(S, \xi)$ does not change.

The asymptotic behavior of the action for large ξ is important for establishing the convergence of any proposed contour C . This is dominated by the scalar curvature and volume terms in (2.14). On the first sheet we have, for large $|\xi|$,

$$\mathcal{I}(S, \xi) \sim (5\sqrt{2}/8) S_{\text{crit}} (\xi - \frac{1}{4})^{1/2}, \quad (2.25a)$$

$$\mathcal{G}(\xi) \sim (5\sqrt{2}/8)\sqrt{2}(\xi - \frac{3}{8})^{1/2}, \quad (2.25b)$$

where

$$S_{\text{crit}} = (16/\sqrt{2}) [2\pi - 3 \cos^{-1}(\frac{1}{3})] = 29.306. \quad (2.26)$$

Thus

$$\mathcal{F}(S, \xi) \sim (5\sqrt{2}/8)\sqrt{2}S(S - S_{\text{crit}})\xi^{1/2}. \quad (2.27)$$

The asymptotic behavior on the first sheet thus depends crucially on whether S is greater or less than the critical value S_{crit} . On other sheets the asymptotic behavior will change as the branch points at $\xi = \frac{1}{4}$ and $\frac{3}{8}$ are circled, resulting in changes of signs of the factors in (2.25).

III. SEMICLASSICAL APPROXIMATIONS

The wave function defined by (2.19) will predict classical space-time for those values of S and H for which the semiclassical approximation appropriate to Lorentz signatured classical geometries is valid. In this section we explore the classical geometries predicted by the action (2.14) and the semiclassical approximations which can be built upon them.

Classical simplicial geometries are the extrema of the Regge action, here determined by the single algebraic equation

$$I'(S, \xi) = 0, \quad (3.1)$$

where a prime denotes the derivative with respect to ξ . For a given boundary edge length, Eq. (3.1) is to be solved for the value of ξ that extremizes the action. This extremum determines the interior edges through (2.8) and thus a complete simplicial geometry. From (2.14), condition (3.1) is equivalent to

$$S = \mathcal{F}'(\xi)/\mathcal{G}'(\xi), \quad (3.2)$$

a relation which permits an easy graphical analysis of the extrema. The left-hand side of (3.2) is real. The right-hand side of (3.2) is real for real $\xi > \frac{3}{8}$ because both \mathcal{F} and \mathcal{G} are real and real for real $\xi < \frac{1}{4}$ because they are purely imaginary. The same right-hand side is reached whether one continues to above or below the cut $\xi < \frac{1}{4}$. Figure 2 shows a plot of the right-hand side of (3.2). From (2.25) asymptotically for large ξ one has

$$\mathcal{F}'(\xi)/\mathcal{G}'(\xi) \sim S_{\text{crit}}, \quad (3.3)$$

where S_{crit} is given by (2.26). Thus for every $0 < S < S_{\text{crit}}$ there is a Euclidean geometry with $\xi > \frac{3}{8}$, which is a solution. For every $S > S_{\text{crit}}$ there is a Lorentzian geometry with $\xi < \frac{1}{4}$, which is a solution.

The real solutions of (3.2) correspond to *pairs* of extrema of the action. For $S > S_{\text{crit}}$, $\xi < \frac{1}{4}$ the two extrema are reached from $\xi > \frac{3}{8}$ by continuing to either above the cut along $\xi < \frac{1}{4}$ or to below it. The action of both these extrema is purely imaginary [cf. (2.24)], but of opposite sign. For $S < S_{\text{crit}}$ there is an extremum on the first sheet with $\xi > \frac{3}{8}$ and a real Euclidean action. The second member of the pair is at the same location on the second sheet, reached by continuing around all the branch points at $\xi = \frac{1}{4}$, $\frac{1}{2}$, and $\frac{3}{8}$. It also has real action, but of opposite sign. As S is varied smoothly from below S_{crit} to above it, this pair of extrema migrate to ever larger values of real ξ and reappear as the two extrema with

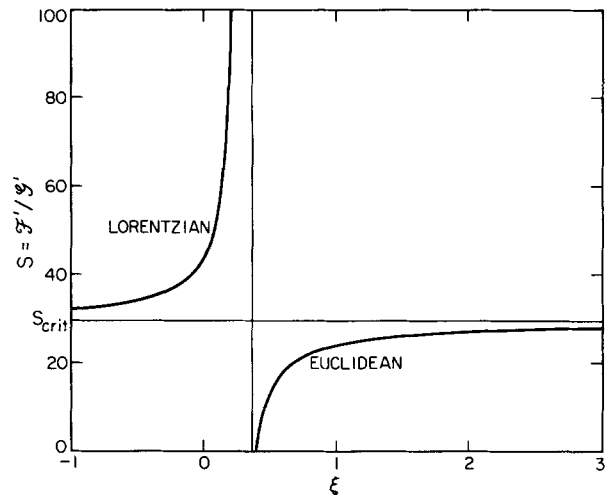


FIG. 2. Classical solutions. The solution of the algebraic equation that determines the extrema of the Euclidean Regge action can be obtained from the curve plotted here. It is a plot of the function $\mathcal{F}'(\xi)/\mathcal{G}'(\xi)$, which is equal to the scaled squared boundary edge length S at an extremum. A value of S thus determines ξ and a unique squared interior edge length through $s_i = H^2 l^2 \xi / S$. For $S < S_{\text{crit}}$ the solutions have $\xi > \frac{3}{8}$, real action, and Euclidean signature. For $S > S_{\text{crit}}$ the solutions have $\xi < \frac{1}{4}$, imaginary Euclidean action, and Lorentzian signature.

$S > S_{\text{crit}}$ at large negative ξ .

It is interesting to compare the distribution of extrema obtained here with those of the analogous continuum minisuperspace model in which the geometries are restricted to be homogeneous and isotropic.² There the solution of the Euclidean Einstein equation with cosmological constant is a round four-sphere with radius H^{-1} . There are real Euclidean solutions for round three-sphere boundaries whose boundary radius is less than the critical value H^{-1} . In the continuum model there are *two* solutions for a boundary radius less than H^{-1} corresponding to a four-geometry consisting of greater than a hemisphere of the four-sphere or less than a hemisphere. The action (2.2) is negative for both. However, because of the \sqrt{g} in (2.2), it can be continued in the metric so as to reverse its overall sign. We should, therefore, count *four* extrema of the action in the space of complex metrics—two with positive action and two with negative.

Analogously to the continuum case the simplicial model has real extrema when the boundary is sufficiently small, $S < S_{\text{crit}}$. Unlike the continuum case there are two extrema of opposite sign of the action rather than four. A model with a single interior vertex is incapable of approximating both more than a hemisphere of a four-sphere and less.

For boundary radii greater than H^{-1} the continuum model exhibits two pairs of extrema. Each pair has complex conjugate values of the action. The pairs differ in the sign of the real part of the action. The imaginary parts are the action of Lorentzian de Sitter space normalized to vanish at the minimum radius of contraction. For $S > S_{\text{crit}}$ the simplicial model displays two extrema with purely imaginary complex conjugate actions.

The wave function (2.19) will predict the correlations of classical space-time where it is well approximated by the semiclassical approximation associated with one or both of the Lorentzian extrema. This will be the case when the con-

tour C can be distorted to pass as a steepest descents contour through these points and the range of integration in their neighborhoods gives the dominant contribution to the integral. For this to be the case S and H must be such that, locally, the integrand is sharply peaked about the extrema. Globally the contour must be such that no greater contributions arise from other extrema on the steepest descents contour or its end points.

Semiclassical approximations for $\Psi_0(S)$ that predict classical geometry are therefore linear combinations of the steepest descents approximation to the integral (2.19) arising from the Lorentzian extrema. That is, defining $\mathcal{S} = i\mathcal{I}$ so that \mathcal{S} is real at a Lorentzian extremum, such semiclassical approximations are linear combinations of

$$\Psi_0(S) \sim \left[\frac{S^2}{2\pi H^2 \mathcal{S}''_{\text{ext}}(S)} \right]^{1/2} \times \exp \left\{ \pm i \left[\frac{\mathcal{S}_{\text{ext}}(S)}{H^2} - \frac{\pi}{4} \right] \right\}, \quad (3.4)$$

where \mathcal{S}_{ext} and $\mathcal{S}''_{\text{ext}}$ are evaluated at the extremum value of ξ . For the CPT symmetric wave function of the no boundary proposal we expect the real combination of these two exponentials.

If the local and global properties of the contour are appropriate as described above, we expect the steepest descents approximation to be valid when the argument of the exponentials in (3.4) is large. This will be the case for the large s_b of the late universe, where

$$\mathcal{S}_{\text{ext}}(S)/H^2 \sim \frac{5}{16}(S/H)^2 = \frac{5}{16}(\Lambda s_b^2/l^2); \quad (3.5)$$

it will also be the case over the whole range of S (except for turning points) when $H^2 = l^2\Lambda/3$ is sufficiently small, as it certainly is in our late universe.

IV. STEEPEST DESCENTS CONTOUR FOR THE NO BOUNDARY WAVE FUNCTION

The descending contour of constant imaginary action passing through both complex conjugate extrema for $S > S_{\text{crit}}$ yields a convergent integral defining a real Ψ_0 that predicts classical space-time when H^2 is small. Therefore, it is a natural candidate for the contour defining the no boundary wave function of the universe. In this section we shall demonstrate these results and discuss the continuation of the resulting wave function to values of $S < S_{\text{crit}}$. For the one complex variable of this model, a descending contour of constant imaginary action is a steepest descents contour.

Figure 3 shows the steepest descents contour that passes through both Lorentzian extrema when $S > S_{\text{crit}}$. The contour consists of two complex conjugate sections, each passing through one extremum. Along with the real analyticity of the action, this ensures that the wave function resulting from (2.19) is real. Each section is a curve of constant $\text{Im}(\mathcal{S})$ equal to its value \mathcal{S}_{ext} at the extremum through which it passes. Descending most steeply from the extremum one could generally end either at infinity, a singular point of the function \mathcal{S} , or at another extremum with the same value of $\text{Im}(\mathcal{S})$. The only singular point is at $\xi = \frac{1}{3}$, at which $\text{Im}(\mathcal{S})$ diverges; therefore no steepest descents contour can end there. The two exhibited extrema have opposite

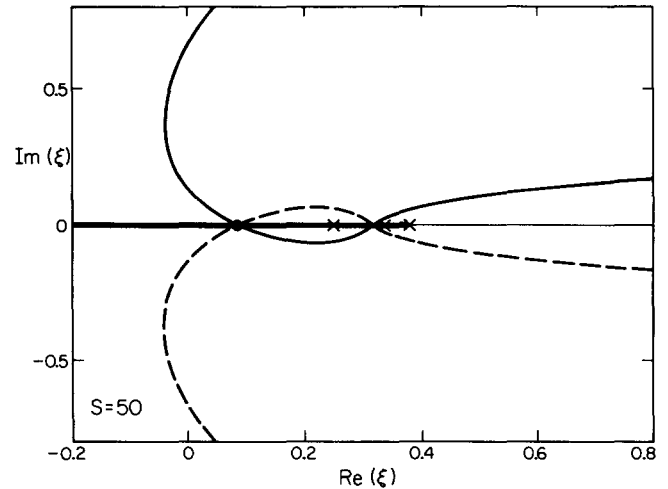


FIG. 3. The steepest descents contour for $S > S_{\text{crit}}$. Shown here is the complex ξ plane with branch points (\times) at $\xi = \frac{1}{3}$, $\frac{1}{3}$, and $\frac{2}{3}$ cut from $-\infty$ to $\frac{2}{3}$. The steepest descents contour for $S = 50$ is plotted. It consists of two complex conjugate sections plotted as the solid and dotted lines. Each passes (on different sheets) through an extremum of the action (\bullet) at $\text{Re } \xi = -0.0836$, $\text{Im } \xi = 0$ and each has infinite end points.

signs of $\text{Im}(\mathcal{S})$ so that a steepest descents contour cannot connect them. In the absence of any other extrema the steepest descents contour must pass from infinity to infinity; the numerical integration of Fig. 3 bears this out. Proceeding upward from the extremum, Eq. (2.27) shows the contour is asymptotic on the first sheet to the parabola

$$(5\sqrt{2}/8)S(S - S_{\text{crit}})\text{Im}(\xi^{1/2}) = \mathcal{S}_{\text{ext}}. \quad (4.1)$$

Along this curve the asymptotic behavior of $\text{Re}(\mathcal{S})$ is

$$\text{Re } \mathcal{S}(S, \xi) \sim (5\sqrt{2}/8)(S - S_{\text{crit}})|\xi|^{1/2}, \quad (4.2)$$

so that the defining integral (2.19) converges with any polynomial measure. Proceeding downward from the extremum the contour enters the second sheet. It cannot proceed directly to infinity since the action is asymptotically negative on the second sheet. Rather, for sufficiently large S the contour passes through the cut between $\xi = \frac{1}{3}$ and $\frac{2}{3}$ reaching a third sheet, in effect changing the asymptotic sign of \mathcal{S} , but not of \mathcal{S} . On this third sheet the contour proceeds to infinity along the parabola

$$(5\sqrt{2}/8)(S + S_{\text{crit}})\text{Im}(\xi^{1/2}) = \mathcal{S}_{\text{ext}}. \quad (4.3)$$

$\text{Re } \mathcal{S}$ behaves as

$$\text{Re } \mathcal{S}(S, \xi) \sim (5\sqrt{2}/8)(S + S_{\text{crit}})|\xi|^{1/2} \quad (4.4)$$

and the integral from infinity to infinity is therefore convergent. For smaller values of S the behavior near the branch points is slightly more complicated, but the contour is still infinite in extent. Since each section of the contour has no finite end points or other extrema along it, as \mathcal{S} becomes large or H^2 small the behavior of integral (2.19) along each section is given increasingly accurately by the steepest descents approximation based on the Lorentzian extremum. Thus taking both sections of the contour together, the semiclassical approximation for $S > S_{\text{crit}}$ becomes

$$\Psi_0(S) \sim \left[\frac{S^2}{2\pi H^2 \mathcal{I}''_{\text{ext}}(S)} \right]^{1/2} 2 \cos \left[\frac{\mathcal{I}''_{\text{ext}}(S)}{H^2} - \frac{\pi}{4} \right]. \quad (4.5)$$

Thus we recover a real Ψ_0 and classical space-time when the universe is large.²³

The third sheet, reached by following the steepest descents contour downward from the extremum reached from the upper half of the first sheet, is the same as that reached from following the steepest descents contour upward from the extremum reached from the lower half of the first sheet. It is this crucial fact that allows the closure of the contour and a simple analytic continuation of integral (2.19) to $S < S_{\text{crit}}$. The fact may be deduced from an elementary, but detailed analysis of the change in phases of the various terms in (2.14) as one proceeds along the contour. A more general argument is as follows: We are considering the two continuations $\mathcal{I}_I(\xi)$ and $\mathcal{I}_{II}(\xi)$ along complex conjugate curves. Initially, on the first sheet, as a consequence of real analyticity, the continuations are related by $\mathcal{I}_I(\xi) = \overline{\mathcal{I}_{II}(\xi)}$; this relation will continue to be maintained because the contours are conjugate to each other. Therefore if the continuations cross the real axis in a range where each are separately real, we have

$$\mathcal{I}_I(\xi) = \overline{\mathcal{I}_{II}(\xi)} = \mathcal{I}_{II}(\xi) \quad (4.6)$$

and they will agree. However, no matter how the branch point are circled, $\mathcal{I}(\xi)$ is real for $\xi > \frac{3}{8}$. Circling one of the square root branch points can at most change its sign. Circling the logarithmic branch point changes $\cos^{-1}(z) \rightarrow \cos^{-1}(z) \pm \pi$. Therefore the two continuations must reach a common third sheet.

The asymptotic behaviors (4.2) and (4.4) allow the two sections of the steepest descents contour to be joined at infinity on the first and third sheets. The result is a closed contour defining the wave function of the universe. The contour can be distorted smoothly from the third sheet to the second because $\mathcal{I}(\xi)$ is not singular at the branch point $\xi = \frac{3}{8}$ through which it passes. The result is the closed contour of Fig. 4.

Since the contour is closed and finite, there is no obstacle to continuing the wave function defined by (2.19) to values of S less than S_{crit} . One can then investigate the semiclassical behavior of Ψ_0 in the limit where H^2 becomes small. In fact, the contour can be distorted into a steepest descents contour for $S < S_{\text{crit}}$. The extrema are located at real values of ξ on the first and second sheets. The asymptotic behavior of (2.19) for small H^2 is given by the integral in the neighborhood of the extremum on the first sheet. This is

$$\Psi_0(S) \sim - [S^2/2\pi H^2 I''_{\text{ext}}(S)]^{1/2} \exp[-I_{\text{ext}}(S)], \quad (4.7)$$

where $I_{\text{ext}}(S)$ and $I''_{\text{ext}}(S)$ are evaluated at the extremum value of ξ .

With the contour defined, both the integral (2.19) and its semiclassical approximations (4.5) and (4.7) are easily evaluated. Figure 5 shows a numerical evaluation of Eq. (2.16) for $H^2 = 50$ along the actual steepest descents contour. Figure 6 shows the corresponding semiclassical approximation evaluated from (4.5) and (4.7). For this value

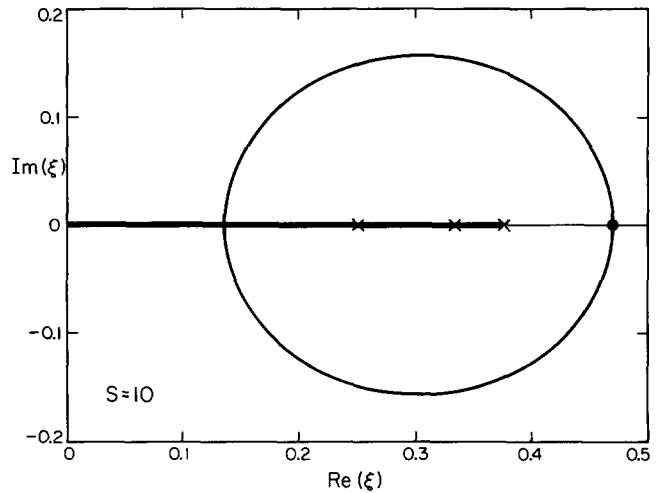


FIG. 4. Continuation to $S < S_{\text{crit}}$. The steepest descents contour shown in Fig. 3 can be distorted into the closed contour shown. Starting on the positive real axis the contour winds around all finite branch points, through the cut $-\infty < \xi < \frac{3}{8}$, onto the second sheet, and around all the finite branch points again to close on the first sheet. Thus it winds around the branch points *twice* on the curve shown. Using the closed contour the integral can be continued to $S < S_{\text{crit}}$. For these values the integral can be distorted into a steepest descents contour, shown here for $S = 10$. This contour passes through both real extrema (●) at $\text{Re } \xi = 0.469$, $\text{Im } \xi = 0$, one on the first sheet, one on the second. It is the integral on the first sheet that gives the dominant contribution to the integral defining the wave function in the semiclassical approximation.

of H^2 , $\mathcal{I}/H^2 \gtrsim 20$ in the classical allowed region $S > S_{\text{crit}}$, so that we expect the semiclassical approximation to give a good approximation to the actual integral. It does for large values of S . The semiclassical approximation gives a poor approximation for S near S_{crit} and only a moderate approximation below S_{crit} .

Both the wave function and its semiclassical approximation show the characteristic features expected from similar minisuperspace models based on symmetry.² Here, $S > S_{\text{crit}}$ is the classically allowed region in which the wave function

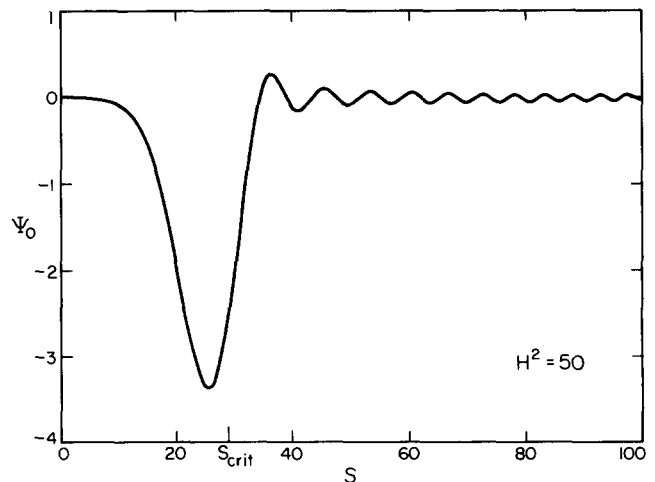


FIG. 5. The wave function. A numerical integration of the wave function defined by Eq. (2.19) and the steepest descents contour of Figs. 3 and 4 is plotted for $H^2 = 50$. The wave function oscillates in the classically allowed range of $S > S_{\text{crit}}$. In the classically forbidden range of $S < S_{\text{crit}}$ the wave function decays inward from the very large peak in $|\Psi_0|$ at S_{crit} .

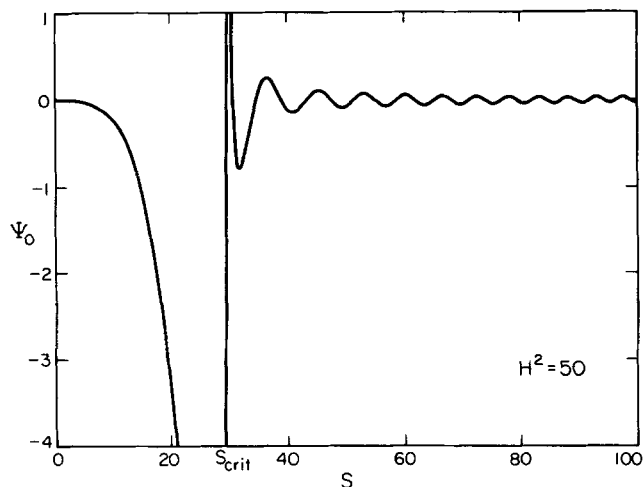


FIG. 6. The semiclassical wave function. The semiclassical approximation to the wave function specified by Eqs. (4.5) and (4.7) is plotted for $H^2 = 50$. The semiclassical approximation is infinite at the "turning point" $S = S_{\text{crit}}$ because $I''_{\text{ext}}(S)$ vanishes there. The semiclassical wave function becomes an increasingly accurate approximation to the wave function of Fig. 4 for large values of S . Where this approximation is valid we may say that the wave function predicts the correlations of classical de Sitter space.

oscillates. The semiclassical approximation here corresponds to classical de Sitter space. The oscillation at arbitrarily large values of S corresponds to the limitless expansion of de Sitter space. The boundary between the classically allowed and classically forbidden regions at $S = S_{\text{crit}}$ corresponds to the minimum radius of contraction H^{-1} . The wave function is large near the boundary S_{crit} , corresponding to the most probable three spheres in de Sitter space. It decays exponentially from these high values for $S < S_{\text{crit}}$, reflecting the classically forbidden nature of this region.

V. CONCLUSIONS

The steepest descents contour for the no boundary wave function of the universe explicitly displayed in this paper manifestly meets two of the criteria set forth in Sec. I. It leads to a convergent integral for Ψ_0 and to a wave function that predicts classical space-time when the universe is large. The third criterion, which concerned the constraints implementing diffeomorphism invariance, cannot be an issue for this simple Regge model since a simplicial geometry exhibits no exact nontrivial invariances, but only approximate ones (see, e.g., Ref. 18).

The proposed contour is in no sense a distortion or rotation of the contour of integration over real Euclidean geometries. That contour runs along the real ξ axis from $\xi = \frac{2}{3}$ to $\xi = \infty$. Therefore, it has a finite end point at $\xi = \frac{2}{3}$ that will not be displaced by distortion or rotation. For $S > S_{\text{crit}}$ the integral (2.19) over this real contour converges. However, the asymptotic behavior for small H^2 is not governed by a Lorentzian extremum, but rather by the end point at $\xi = \frac{2}{3}$. The wave function defined by this contour does not predict classical space-time in the late universe.

The results of this model suggest that it will be of considerable interest to investigate whether a descending contour of constant imaginary action through the classical extrema can provide a general definition of the no boundary wave

function consistent with convergence, classical space-time, and invariance.

ACKNOWLEDGMENT

Thanks are due to D. Page and J. Halliwell for constructive criticism.

This work was supported in part by the National Science Foundation under Grant No. PHY 85-06686.

¹S. W. Hawking, in *Astrophysical Cosmology: Proceedings of the Study Week on Cosmology and Fundamental Physics*, edited by H. A. Brück, G. V. Coyne, and M. S. Longair (Pontificae Academiae Scientiarum Scripta Varia, Vatican City, 1982); Nucl. Phys. B **264**, 185 (1984).

²J. B. Hartle and S. W. Hawking, Phys. Rev. D **28**, 2960 (1983).

³S. W. Hawking, Phys. Scr. T **15**, 151 (1987).

⁴S. Coleman (to be published); S. Giddings and A. Ströminger (to be published).

⁵See, e.g., J. B. Hartle, in *Proceedings of the Osgood Hill conference on conceptual problems of quantum gravity* (to be published) or *Proceedings of the 5th Marcel Grossmann conference on recent developments in general relativity* (to be published).

⁶See, e.g., J. B. Hartle, Class. Quantum Grav. **2**, 707 (1985).

⁷See, e.g., H. Leutwyler, Phys. Rev. **134**, B1155 (1964); B. S. DeWitt, in *Magic Without Magic: John Archibald Wheeler*, edited by J. Klauder (Freeman, San Francisco, 1972); E. Fradkin and G. Vilkovisky, Phys. Rev. D **8**, 4241 (1973); L. Faddeev and V. Popov, Usp. Fiz. Nauk **111**, 427 (1973); M. Kaku, Phys. Rev. D **15**, 1019 (1977); C. Teitelboim, *ibid.* **28**, 310 (1983); H. Hamber, in *Critical Phenomena, Random Systems and Gauge Theories: Les Houches 1984*, edited by R. Stora and K. Osterwalder (Elsevier Sciences, Amsterdam, 1986); M. Bander, Phys. Rev. Lett. **57**, 1825 (1986).

⁸See, e.g., B. DeWitt, Phys. Rev. **160**, 571 (1967); U. Gerlach, Phys. Rev. **177**, 1929 (1969); V. Lapchinsky and V. Rubakov, Acta Phys. Polonica B **10**, 1041 (1979); T. Banks, Nucl. Phys. B **249**, 332 (1985); J. Halliwell and S. W. Hawking, Phys. Rev. D **31**, 1777 (1985). There are many later references.

⁹C. Teitelboim, Phys. Rev. Lett. **50**, 705 (1983); J. Halliwell (to be published).

¹⁰G. Gibbons, S. W. Hawking, and M. Perry, Nucl. Phys. B **138**, 141 (1978).

¹¹J. B. Hartle, Phys. Rev. D **29**, 2730 (1984); J. B. Hartle and K. Schleich, in *Quantum Field Theory and Quantum Statistics*, edited by T. A. Batalin, C. J. Isham, and G. A. Vilkovisky (Adam Hilger, Bristol, 1987); H. Ari-sue, T. Fujiwara, M. Kato, and K. Ogawa, Phys. Rev. D **35**, 2309 (1987); D. Boulware (unpublished).

¹²K. Schleich, Phys. Rev. D **36**, 2342 (1987).

¹³R. Schoen and S.-T. Yau, Phys. Rev. Lett. **43**, 1457 (1979); E. Witten, Commun. Math. Phys. **80**, 381 (1987).

¹⁴R. Schoen and S.-T. Yau, Phys. Rev. Lett. **42**, 547 (1979).

¹⁵For reviews of some of the earlier literature on the application of minisuperspace methods to canonical quantum gravity, see C. W. Misner, in *Magic Without Magic: John Archibald Wheeler*, edited by J. Klauder (Freeman, San Francisco, 1972); M. Ryan, *Hamiltonian Cosmology* (Springer, New York, 1972); M. A. H. MacCullum, in *Quantum Gravity*, edited by C. J. Isham, R. Penrose, and D. Sciama (Clarendon, Oxford, 1975).

¹⁶For a review of some of the earlier applications of minisuperspace to the no boundary proposal see, e.g., J. B. Hartle, in *High Energy Physics 1985: Proceedings of the Yale Theoretical Advanced Study Institute*, edited by M. J. Bowick and F. Gürsey (World Scientific, Singapore, 1986). References to both later and earlier papers can be found in J. J. Halliwell, *Bibliography of Papers on Quantum Cosmology* (to be published).

¹⁷M. Ryan and K. Kuchař, in *Gravitational Collapse and Relativity*, edited by H. Sato and T. Nakamura (World Scientific, Singapore, 1986).

¹⁸J. B. Hartle, J. Math. Phys. **26**, 804 (1985) (referred to as paper I).

¹⁹T. Regge, Nuovo Cimento **19**, 558 (1961).

²⁰J. B. Hartle, *J. Math. Phys.* **27**, 287 (1986) (referred to as paper II).

²¹For the boundary term see J. B. Hartle and R. Sorkin, *Gen. Relat. Gravit.* **13**, 541 (1981).

²²See, e.g., C. Teitelboim, *Phys. Rev. D* **25**, 3159 (1983); **28**, 297, 310 (1983); J. B. Hartle, in *Gravitation in Astrophysics*, edited by B. Carter and J. B. Hartle (Plenum, New York, 1987); J. B. Hartle, *Phys. Rev. D* **37**, 2818 (1988); J. B. Hartle (to be published).

²³By taking only a single section of the contour we would recover a wave function that in the semiclassical limit behaves like $\exp(i\mathcal{S}_{\text{ext}}/H^2)$ in the classically allowed region; possessing "outgoing waves," it is analogous to the "tunneling" wave function of A. Vilenkin [*Phys. Lett. B* **117**, 25 (1983); *Phys. Rev. D* **27**, 2848 (1983); **30**, 509 (1984); **37**, 2872 (1988)]. However, we have not investigated the continuation of this wave function to $\mathcal{S} < \mathcal{S}_{\text{crit}}$.